Preprint
UCRL-JC-145023

Cloud-Resolving Model Intercomparison with the ARM Summer 1997 IOP Data

K.-M. Xu, D. E. Johnson, W.-K. Tao, S. K. Krueger, M. Khairoutdinov, D. A. Randall, L. J. Donner, C. J. Seman, J. C. Petch, F. Guichard, R. T. Cederwall, S. C. Xie, J. J. Yio, W. Grabowski, M.-H. Zhang

This article was submitted to
10th Atmospheric Radiation Measurement Science Team Meeting, San Antonio, TX, March 13-17, 2000

March 13, 2000

This work was performed under the auspices of the United States Department of Energy by the University of California, Lawrence Livermore National Laboratory under contract No. W-7405-Eng-48.

Cloud-Resolving Model Intercomparison with the ARM Summer 1997 IOP Data

K.-M. Xu
National Aeronautics and Space Administration
Langley Research Center
Hampton, Virginia

S. K. Krueger
University of Utah
Salt Lake City, Utah

L. J. Donner and C. J. Seman
National Oceanic and Atmospheric Administration
Geophysical Fluid Dynamics Laboratory
Princeton, New Jersey

F. Guichard
Centre National de Recherches Meteorologiques
France

W. Grabowski
National Center for Atmospheric Research
Boulder, Colorado

D. E. Johnson and W.-K. Tao
National Aeronautics and Space Administration
Goddard Space Flight Center
Greenbelt, Maryland

M. Khairoutdinov and D. A. Randall
Colorado State University
Fort Collins, Colorado

J. C. Petch
The Met Office
Bracknell, United Kingdom

R. T. Cederwall, S. C. Xie, and J. J. Yio
Lawrence Livermore National Laboratory
Livermore, California

M.-H. Zhang
State University of New York
Stony Brook, New York

Introduction

The Atmospheric Radiation Measurement (ARM) Program's Single Column Model (SCM) working group conducted its intercomparison study of midlatitude summertime continental convection using the July 1995 Intensive Operational Period (IOP) data set (Ghan et al. 2000). Only one cloud-resolving model (CRM) participated in the study. On the other hand, several CRMs participated in the GEWEX (Global Energy and Water-cycle Experiment) Cloud System Study (GCSS) Working Group 4's intercomparison study of tropical deep convection (Krueger and Lazarus 1998; Redelsperger et al. 2000). Both groups decided to have a joint intercomparison project to maximize the resources and advance our understanding of midlatitude continental convection. This joint project compares the cloud-resolving and single-column simulations of summertime continental cumulus convection observed at the Southern Great Plains (SGP) Cloud and Radiation Testbed (CART) site during the ARM Summer 1997 IOP. This paper reports the findings and results of cloud-resolving simulations, while Cederwall et al. (2000) reports the SCM part of the project. Seven CRMs are participating in this project: CNRM, CSU_3d, EULAG, GCE, GFDL, UCLA/CSU, and UKLEM (Table 1).

Table 1. Participated cloud-resolving models in the intercomparison project.

Acronym	Institution	Principal Modeler(s)
CNRM	Centre National de Recherches Meteorologiques	Guichard
CSU-3d	2-D and 3-D Colorado State University	Khairoudinov
EULAG	EUlerian/semi-LAGrangian cloud model	Grabowski
GCE	NASA Goddard cumulus ensemble model	Tao, Johnson
GFDL	NOAA Geophysical Fluid Dynamics Laboratory	Donner, Seman
UCLA/CSU	UCLA/CSU cumulus ensemble model	Xu
UKLEM	2D and 3-D UK Met Office large-eddy model	Petch

Although these CRMs differ significantly in their treatments of cloud microphysics, radiation, and turbulence closures, they all explicitly resolve cloud-scale dynamics. The majority of them participated in an earlier intercomparison study of tropical deep convection observed during the Tropical Ocean-Global Atmosphere (TOGA) Coupled Ocean-Atmosphere Response Experiment (COARE) (Krueger and Lazarus 1998; Redelsperger et al. 2000). Most of them have not been used to simulate midlatitude continental convection with an observed large-scale data set.

The goals of this intercomparison study are to: (1) compare CRM simulations with the detailed cloud parameter observations; (2) compare the performance of CRMs in simulating midlatitude convection with that of tropical convection; and (3) provide detailed analyses of results for improving the representations of cloud processes in general circulation models (GCMs).

Three subcases with convective precipitation events of 4- to 5-day durations were simulated by all seven models using (1) the observed large-scale advective tendencies of temperature and water vapor mixing ratio, analyzed with a variational method (Zhang and Lin 1997), (2) surface turbulence fluxes observed at the SGP CART site, and (3) prescribed radiative heating rate profiles based upon the European Center for Medium-range Weather Forecasting (ECMWF) forecast model and the observed surface and top-of-the-atmosphere (TOA) radiative fluxes. Use of prescribed radiative heating profiles eliminates the complicated interactions between cloud and radiation, which is one of the major difficulties in an intercomparison study (Krueger and Lazarus 1998; Ghan et al. 2000).

All simulations were performed by two-dimensional (x and z) models except for CSU-3d and UKLEM, which made both two-dimensional (2-D) and three-dimensional (3-D) simulations. The UKLEM performed a 3-D simulation for one of the three subcases only. The domain sizes are approximately 500 km in the horizontal and 20 km in the vertical for 2-D simulations, while they are approximately 250 km x 250 km x 20 km for 3-D simulations. The horizontal grid sizes used in these simulations are 2 km (2-D) or 2 km x 2 km (3-D). The vertical resolution varies from models to models, in the range of 100 m and 1000 m, with stretched coordinates in some models.

The three subcases that have been chosen for this intercomparison study are parts of the 29-day ARM SCM IOP during June to July 1997 (Figure 1): Subcase A: 2330 Universal Time Coordinates (UTC) June 26-30, 1997; Subcase B: 2330 UTC July 7-12, 1997; Subcase C: 2330 UTC July 12-17, 1997.

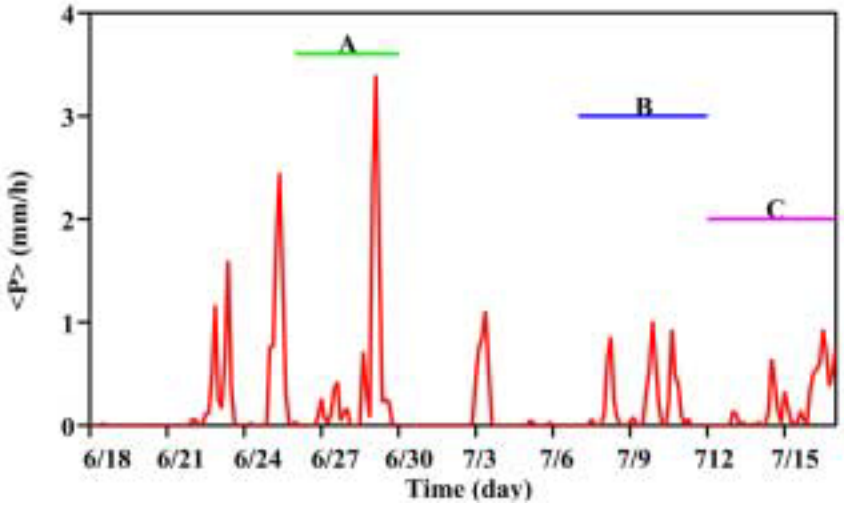

Figure 1. Time series of observed surface precipitation rates during Summer 1997 IOP.

Results

Two types of the intercomparison results are shown in this paper: the subcase time-mean profiles and time series of surface or integrated variables. A brief discussion of the results is presented in this paper. Detailed discussion of the results will be presented in a future journal article.

Temperature and Moisture Profiles

Figures 2, 3, 4, and 5 show the root-mean-square (RMS) errors of CRM simulations relative to observations and the temporal correlation coefficients between the simulated and observed temperature and water vapor mixing ratio, respectively. Observations of temperature and specific humidity profiles are available every 3 h (and somewhat averaged), but simulated data are averaged over 3 h from model outputs saved every 5 or 10 min.

Typical magnitudes of the RMS temperature departures from observations are 1 K to 2 K for Subcase A, and 1 K to 3 K for Subcases B and C, with larger departures in the upper troposphere and the planetary boundary layer (PBL; Figure 2). The observed PBL depths exhibit diurnal variations between 0.2 km and 2.1 km for these three subcases (Krueger et al. 2000). Figure 2 shows that the performance of an individual CRM varies from one subcase to another; for example, CSU_3d, UCLA/CSU, and UKLEM perform rather differently between Subcases A and B. Another feature is the larger intermodel differences above 11 km, which may be related to the weak forcings/small stability, the different model top heights, and different treatments of gravity waves reflections.

The temporal correlation coefficients between the simulated and observed temperature for Subcase B are extremely high below 11 km for all models, i.e., greater than 0.8 (Figure 3). The dominance of temporal variability by the diurnal cycle is partially responsible for this since the net (surface - top of the atmosphere) radiative fluxes are prescribed in the model. In Subcases A and C, however, the correlations are generally much smaller than in Subcase B, and there are larger differences in the

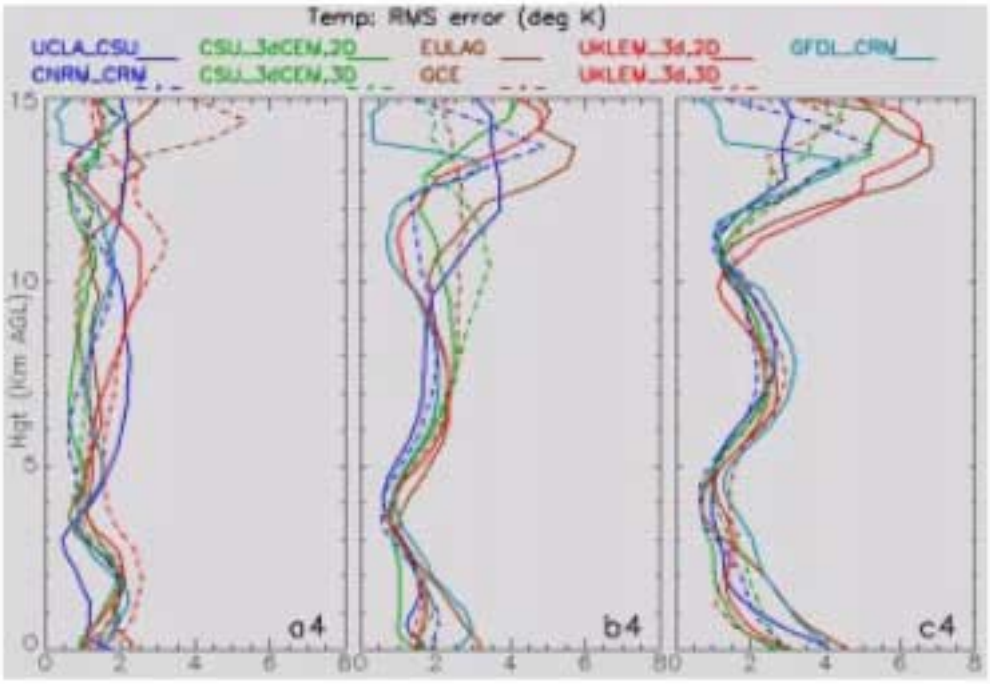

Figure 2. RMS errors of temperature for Subcases A, B, and C.

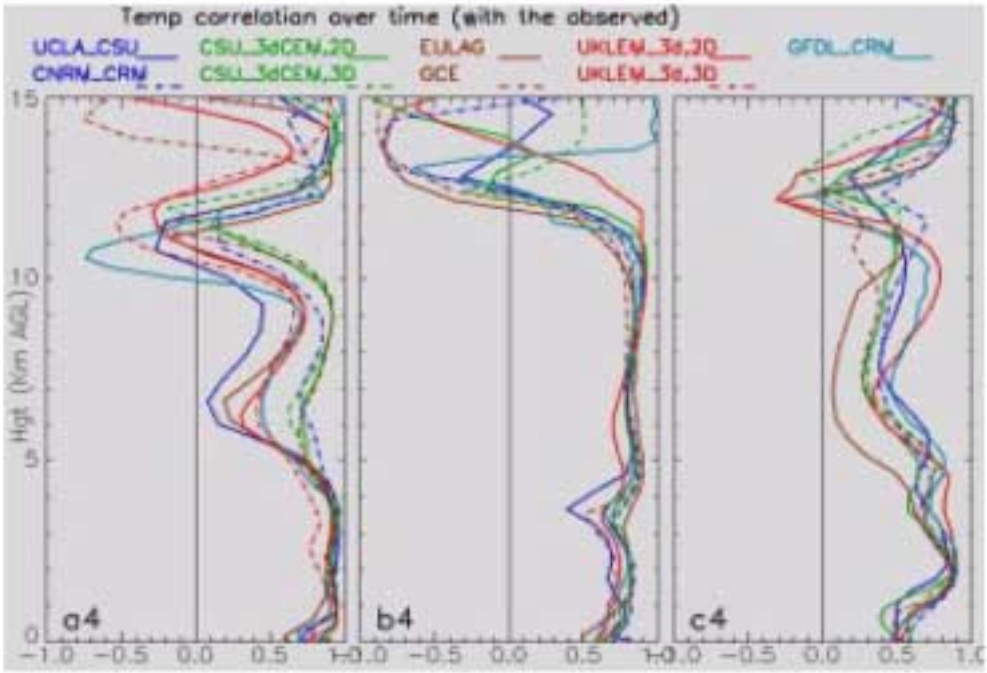

Figure 3. Temporal correlation coefficients of temperature for Subcases A, B, and C.

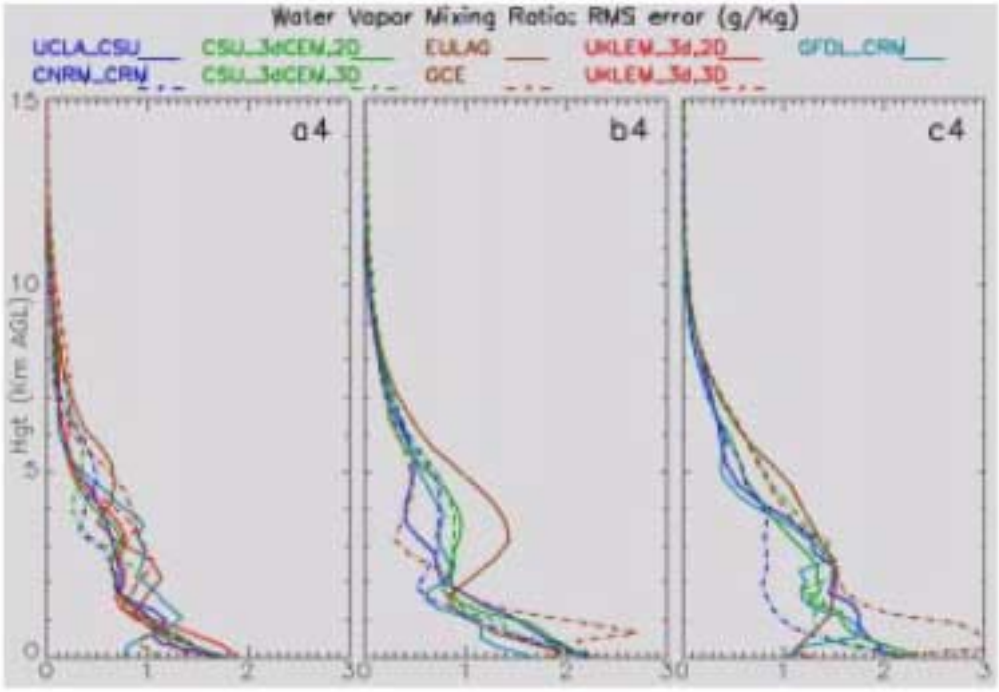

Figure 4. Same as Figure 2 except for water vapor mixing ratio.

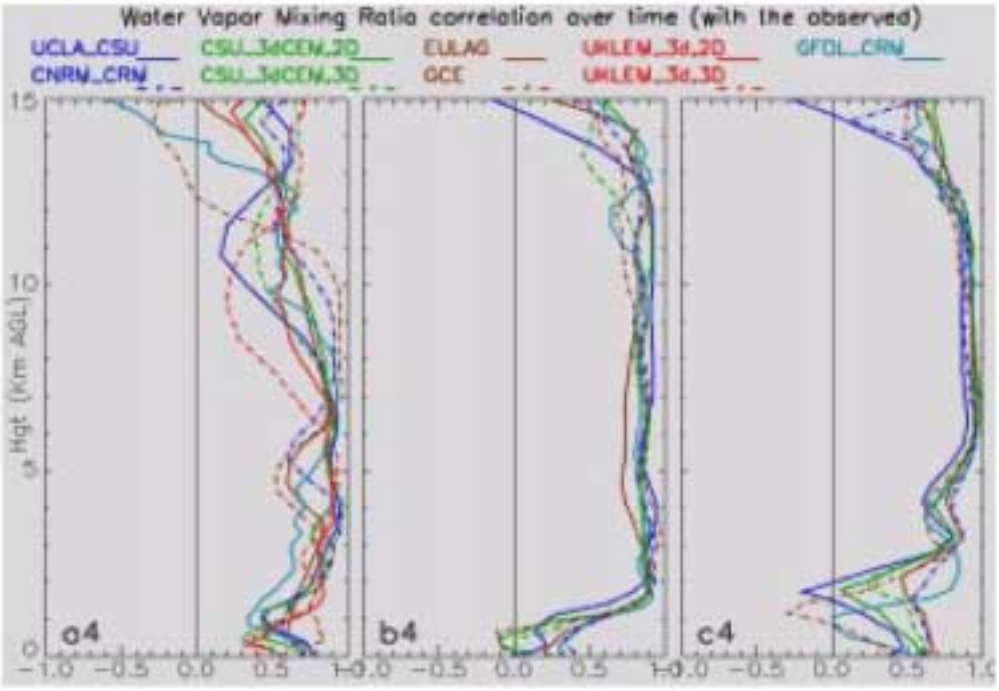

Figure 5. Same as Figure 3 except for water vapor mixing ratio.

correlations among the CRMs. In particular, the correlation coefficients for Subcase A are rather different among the CRMs for the layer above 5 km, in spite of similarly smaller RMS temperature errors than the other two subcases. Therefore, the combination of Figures 2 and 3 give a more comprehensive intercomparison than using either Figure 2 or 3 alone.

In addition, a comparison between 2-D and 3-D simulations from CSU_3-D and UKLEM CRMs shows that the results are very similar (Figures 2 and 3). Little improvement is shown with the third dimension, which is also true for the results shown in the rest of the paper. Such a result may not be surprising because of the small domain sizes used in the simulations with the 3-D versions of the same models. This also justifies the usage of 2-D models in the simulations of the statistical properties of cumulus convection because 2-D models produce similar results as in 3-D models and are computationally more economical (e.g., Grabowski et al. 1998).

The RMS errors of water vapor mixing ratio are larger in the lower troposphere, larger than 1 g kg^{-1} in the PBL, because of its exponential decrease with height (Figure 4). The intermodel differences are not systematic. However, the intermodel differences are about half of the averaged RMS errors among the models. These are proportionally greater than those of temperature, except for Subcase A and the upper troposphere of all subcases (Figure 2). Such a result suggests that the observed moisture variations are more difficult to simulate.

The temporal correlation coefficients between the simulated and observed water vapor mixing ratios show very high values (> 0.7) above 2 km for Subcase B and above 3 km for Subcase C. The intermodel differences are much greater in Subcase A (Figure 5), as in those of temperature (Figure 3). The small correlation coefficients in the PBL are caused by the imposed surface fluxes, i.e., the lack of feedbacks between the surface turbulence fluxes and the thermodynamic variables, possibly the inadequate parameterizations of turbulence in the CRMs, and the time-invariant surface pressure values for each subcase. Sensitivity testing shows that imposing the time-varying, observed surface pressure values in a CRM also slightly improves the overall results of the simulations. The lack of the interactions between surface turbulence fluxes and thermodynamic variables is also important, especially for the water vapor mixing ratio. Simulated specific humidities in the PBL exhibit far greater variabilities than the observed ones (Xu and Randall 2000), which causes larger RMS errors and reduces the temporal correlation coefficients. Uncertainty in the observed surface turbulence fluxes is yet another reason for the larger errors.

Nevertheless, the statistical results of simulated temperature and water vapor mixing ratio from CRMs are, as expected, better than those from SCMs (Krueger and Lazarus 1998; Ghan et al. 2000). The intermodel differences of the temperature, except for upper troposphere, and moisture from observations, are smaller for CRMs, compared to those among the SCMs. The departures from the observations are not much greater than those obtained from an earlier CRM intercomparison study of tropical oceanic convection. The observed variabilities are, however, much greater in the ARM SGP than in the TOGA COARE region. Therefore, the performance of CRMs is acceptable for simulating midlatitude continental convection, relative to that of tropical oceanic convection (Krueger and Lazarus 1998; Xu and Randall 2000).

Time Series

All CRMs basically capture the overall temporal evolutions of surface precipitation rates in Subcases A and B. Most of them, however, have difficulties to simulate the observed temporal evolution of Subcase C (left panels of Figure 6). This is related to the amplitudes of the large-scale advective tendencies, which are large for Subcases A and B, and the accuracy of the advective tendencies, which are not accurate for Subcase C, due to missing of soundings on July 13, 1997 (Julian day 195). Another common feature among the models is that there is a delay for the first precipitating event of all subcases,

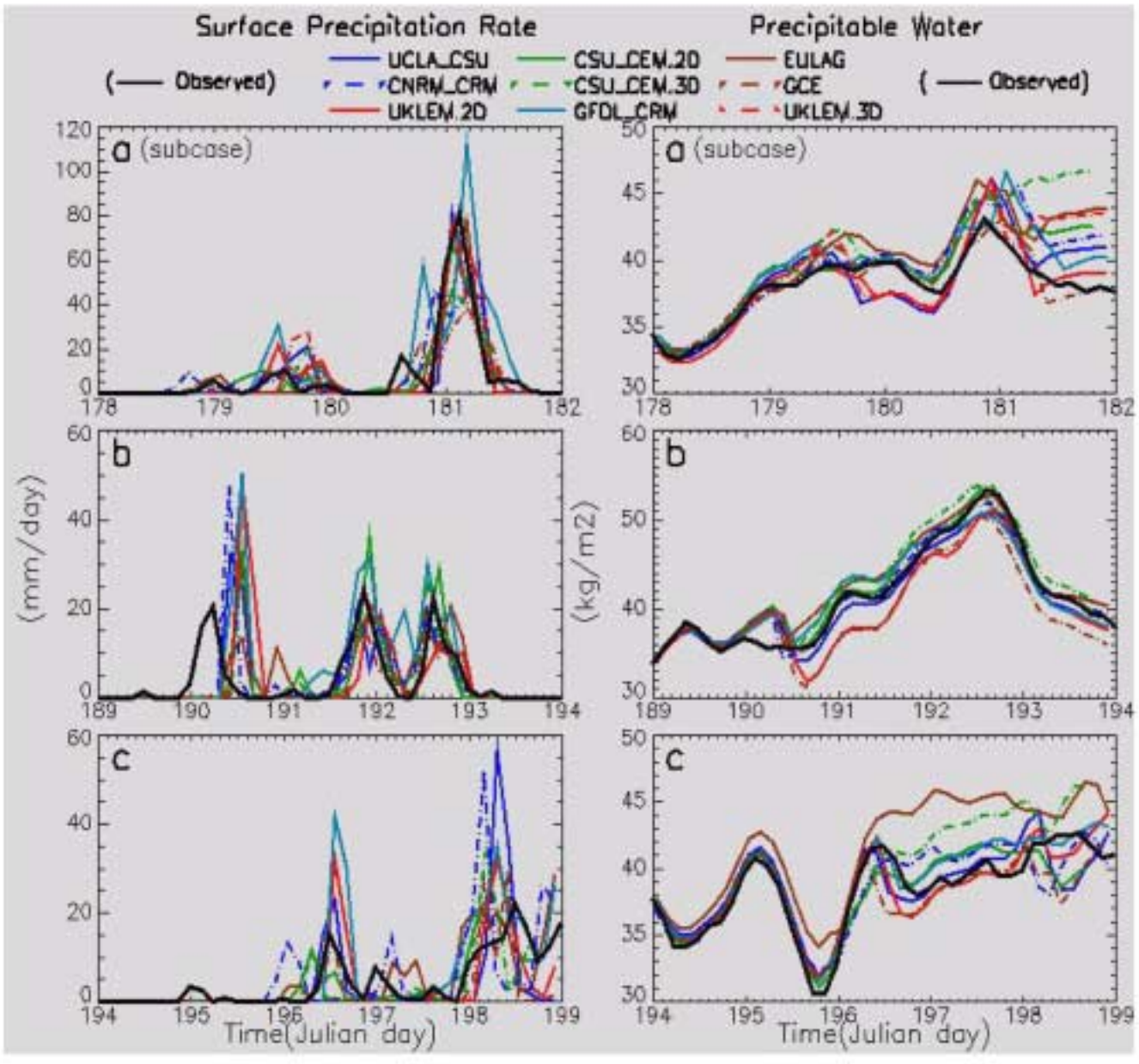

Figure 6. Time series of surface precipitation rates (left) and precipitable water (right panels).

which is most pronounced in Subcase B. This is likely related to the initiation procedure used in all models; that is, models start with horizontally homogeneous soundings with small random perturbations applied to the lowest model layers. This means that initial mesoscale circulations are absent. Without them, CRMs cannot produce precipitation events as promptly as in the observations. SCMs do not possess such a difficulty because triggering of cumulus convection in SCMs is not directly related to mesoscale circulations. The coarse horizontal resolution used in all CRMs may be another possible reason, according to sensitivity tests performed by J. Petch (personal communications, 2000). In addition, one cannot totally eliminate the possibility that inhomogeneous large-scale forcings may improve the simulated timing of precipitation events because the observed cloud systems only occupy a portion of the SGP CART site. That is, the weaker, averaged forcings cannot trigger convection as quickly as in the observations.

The temporal evolutions of precipitable water (right panels of Figures 6), which measures the total vapor mass in a vertical column, show noticeable differences among the models as the model integration time increases. That is, the intermodel differences are smaller than the observed temporal variations. For example, the evolution is rather similar among the models for the first two days of Subcase C, but it diversifies greatly in the last two and a half days. The last day of Subcase A shows the same behavior. Another feature in Figure 6 is that a CRM is consistently drier (UKLEM and GCE) or wetter (CSU_3-D and EULAG) than the observed for all subcases. Differences in rainwater evaporation formulations among the CRMs can account for these differences.

Figure 7 shows the time series of cloud liquid water paths (CLWPs) and column cloud fractions. A novel aspect of this intercomparison study is that the ARM Cloud Working Group provided observations of several cloud properties such as cloud amount, CLWP, and hydrometeor fraction profile, which can be extensively used for intercomparison among CRMs for the first time and provide constraints for the simulated cloud properties.

Left panels of Figure 7 show that most CRMs produce comparable magnitudes of CLWPs to the observed. The CLWPs were measured with a microwave radiometer at the central facility of the CART site (Liljegren 1994), i.e., point measurements of CLWPs. Some corrections were also made to eliminate the contamination by raindrops on the instrument. One of the impacts of this procedure is that the CLWPs are underestimated during intense precipitation events at the central facility, for example, on Julian day 181 of Subcase A.

The temporal evolution of simulated CLWPs (Figure 7) is rather similar to that of surface precipitation rates (Figure 6). The extent of the agreement between the observed and simulated CLWPs varies among the models. That is, the intermodel differences of CLWPs are slightly greater than those of surface precipitation rates. This can be related to the differences in cloud microphysics parameterizations and the different magnitudes of temperature and moisture departures from the observations among the CRMs (Figures 2 and 4). Note that CLWP temporal variations are about 2% of precipitable water variations.

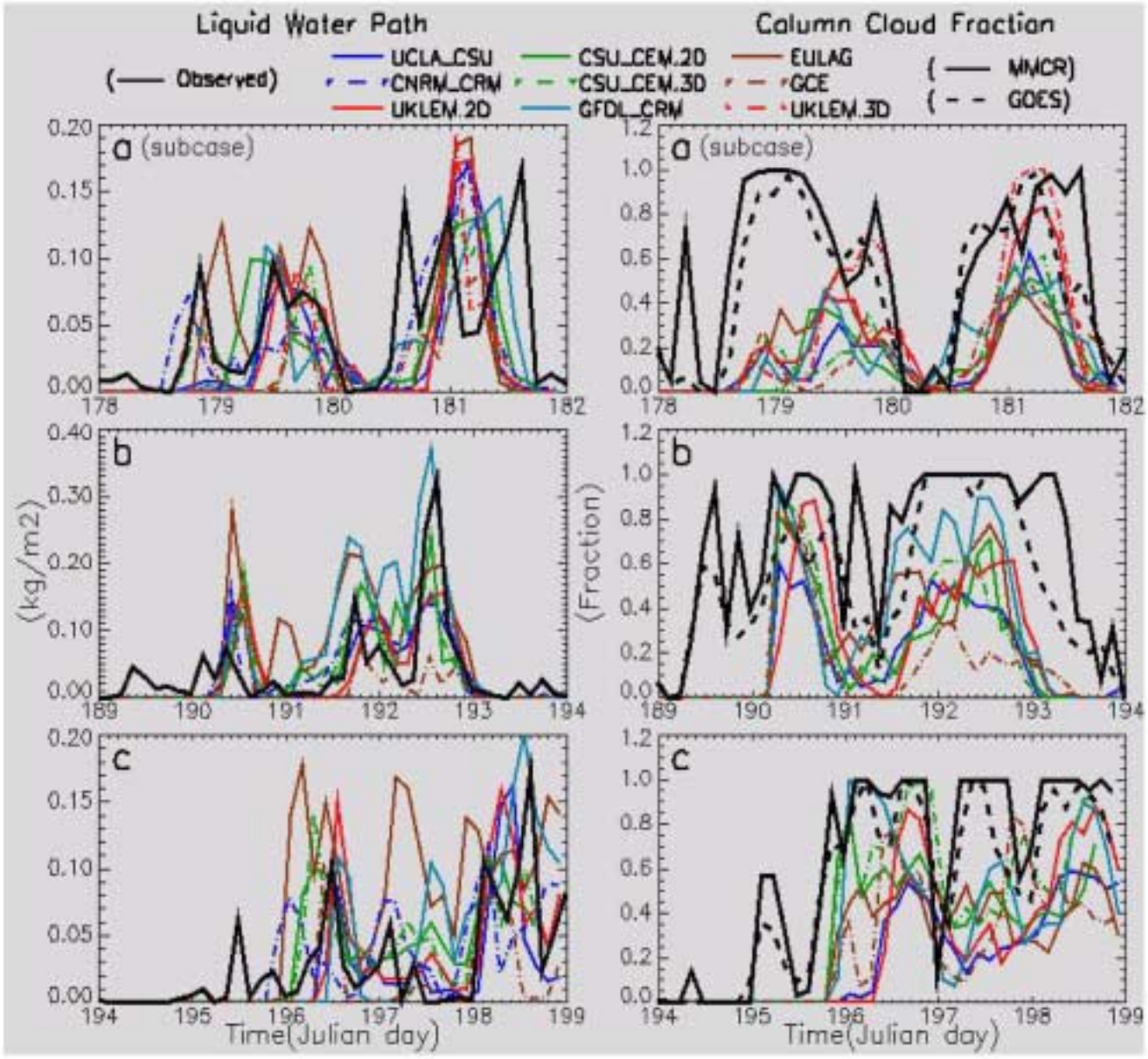

Figure 7. Time series of liquid water path (left) and the column cloud fraction (right panels).

The (total) column cloud fractions (right panels of Figure 7) show even greater differences among the models. The simulated cloud amounts are calculated, based upon grid-column cloud liquid water + ice path exceeding threshold of 0.01 kg m^{-2} (Cahalan et al. 1995; Harshvardhan et al. 1994). This threshold for CRM column cloud fraction diagnosis could be too high to include many observed thin cirrus clouds (Mace et al. 2000). Two observed values of the total cloud fractions are shown in Figure 7, one from satellite observations (GOES-7 satellite; Minnis et al. 1995) and the other from point measurements of ground-based millimeter-wave cloud radar (MMCR; Moran et al. 1997) at the CART central facility. The satellite procedure used the threshold method on the brightness temperature.

Most models show large underestimates, especially in the GCE and UCLA/CSU CRMs (Figure 7). Another common feature among the models is the delay of the development of clouds in the first day of each subcase, due to the lack of initial mesoscale circulations, possibly the coarse horizontal resolution, and the lack of subgrid-scale cloudiness parameterizations used in all models (Xu and Randall 2000). The lack of the agreement in the temporal variations is most likely related to the lack of horizontal hydrometeor advection (Petch and Dudhia 1998). Lack of the third dimension is less likely to be the major cause, but cannot be totally ruled out, e.g., an increase of anvil clouds in the 3-D simulations.

Cloud Property Profiles

The cloud occurrence for a given layer in CRMs is defined, based upon the sum of cloud water and cloud ice mixing ratio over 1% of saturation mixing ratio. The observed curves shown in Figure 8 also include the fractions of precipitating hydrometeors, observed from ground-based point measurements of MMCR at the CART central facility, which are expected to be larger than the cloud occurrences. There is also no guarantee that such measured variables are representative of the subperiod means over the CART region because of inhomogeneous spatial distributions of cloud fields within the CART site.

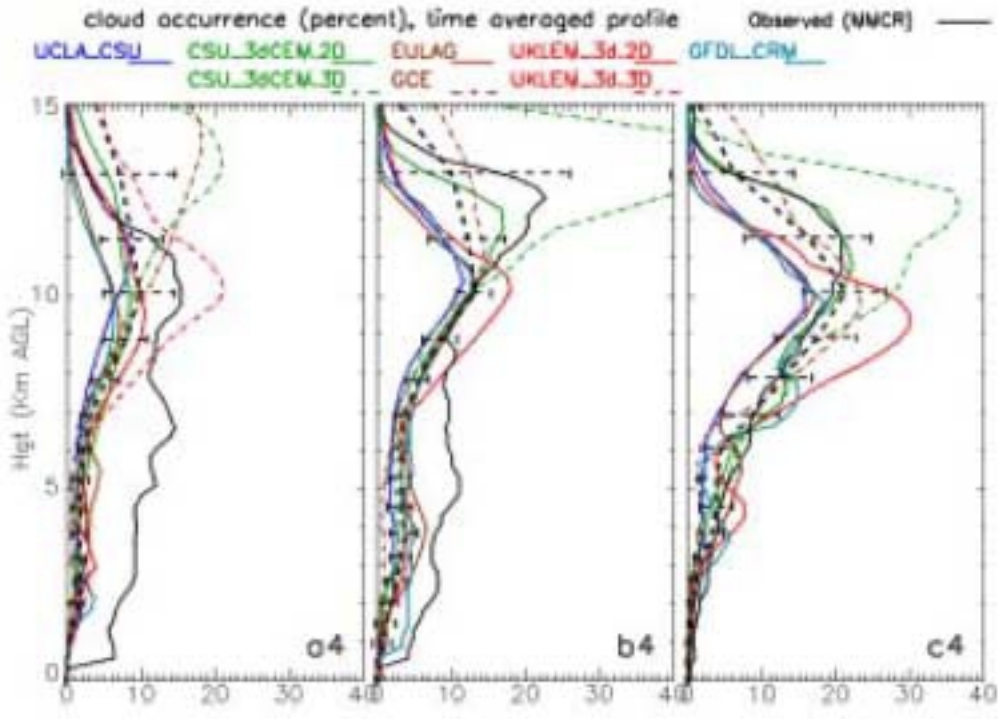

Figure 8. Subcase mean profiles of cloud occurrence for Subcases A, B, and C. Mean and standard deviation of all profiles are also shown.

The intermodel consistency for cloud occurrences among the CRMs is rather good in the lower and middle troposphere, especially for Subcases A and B (Figure 8). That is, the standard deviations from the all-model means (also shown in Figure 8) are rather small in the lower and middle troposphere. The differences of cloud occurrences in the upper troposphere are apparently related to the differences in the ice microphysics parameterizations because warm-phase cloud microphysics parameterizations are more

similar in these CRMs. Three dimensional versions of the UKLEM and CSU_3-D CRMs produce larger cloud fractions than the 2-D counterparts, especially in the upper troposphere. Such a result needs to be further explored with sensitivity tests, using different domain sizes and grid sizes (Tompkins 2000).

The most encouraging result shown in Figure 9 is that most models produce the mean profiles of hydrometeor fractions similar to the observed, although underestimates/overestimates are obvious in Subcase A/C. A comparison between Figures 8 and 9 suggests that the intermodel consistency for the hydrometeor fractions is less than for the cloud occurrences, as indicated by the larger standard deviations from all-model means. Part of the disagreements is related to the small criterion (10^{-6} g g^{-1}) used in defining the precipitating part of hydrometeor fraction. A definition more consistent with the MMCR observations should be adopted in the future in order to give a quantitative comparison. Figure 9 also shows that the 3-D version of CSU_3-D produces greater amounts of hydrometeor fractions than its 2-D counterpart in the upper troposphere. This is also the case in Subcase A for UKLEM. Such a result is, as mentioned earlier, worth further examination because the magnitudes of updraft and downdraft mass fluxes are affected.

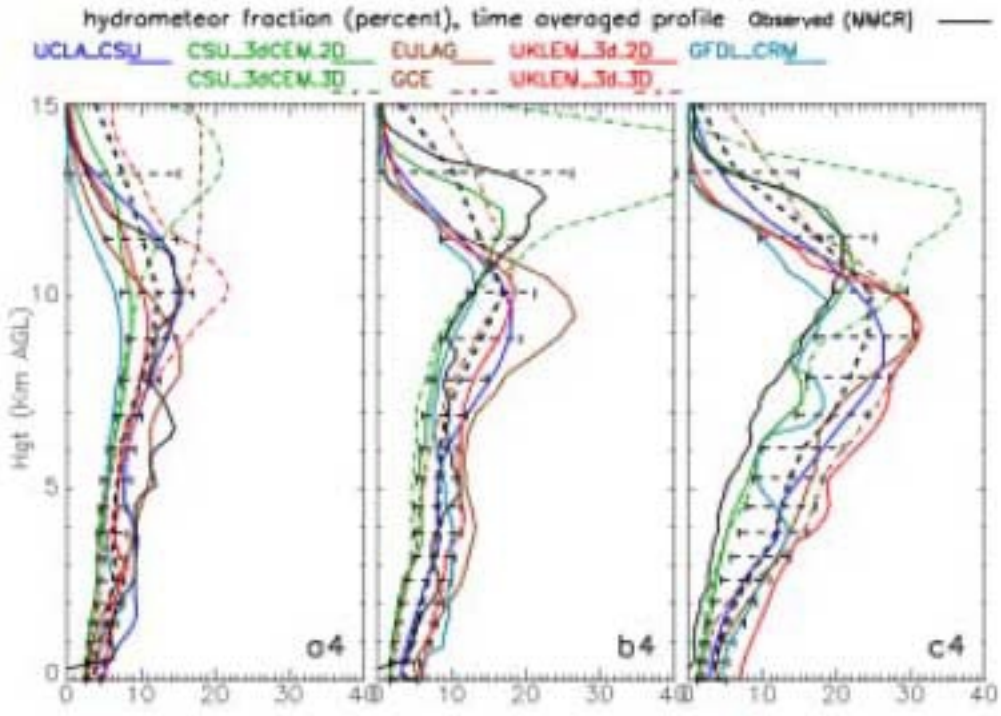

Figure 9. Subcase mean profiles of hydrometeor fractions for Subcases A, B, and C. Mean and standard deviation of all profiles are also shown.

Although most CRMs agree with these cloud property observations reasonably well (Figures 7, 8, and 9), the cloud property observations can be used to evaluate the aspects of the CRMs, for example, cloud microphysics parameterizations used in CRMs, that determine the simulated cloud properties. The cloud-resolving modelers will provide SCMers with detailed analyses of model-generated cloud fields such as the net cloud mass flux (Cederwall et al. 2000), which is the sum of updraft and downdraft mass fluxes (Figure 10), for improvement of parameterizations in SCMs/GCMs.

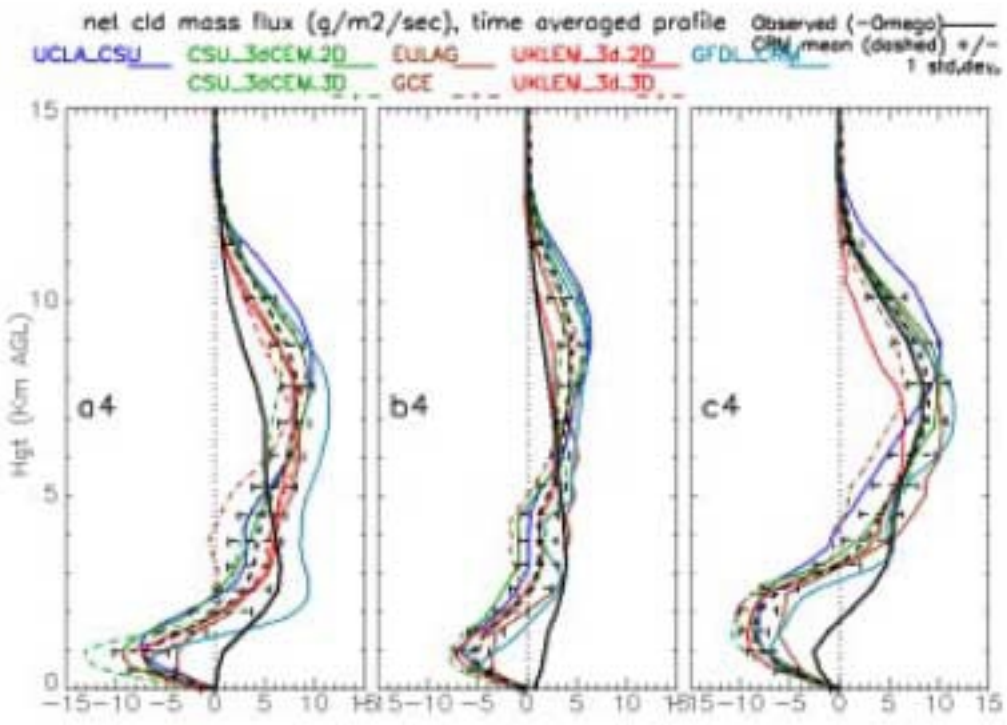

Figure 10. Subcase mean profiles of cloud mass fluxes for Subcases A, B, and C. Mean and standard deviation of all profiles are also shown.

The consistency of the cloud mass fluxes among the models is very good for subcase-mean profiles (Figure 10), but the intermodel differences are not negligible. For comparison, the large-scale mass flux is also shown for each subcase. For Subcases A and B, all models produce subsidence in the environment of the middle and upper troposphere, i.e., cloud mass flux is greater than the large-scale mass flux. This is not the case for the UKLEM for Subcase C. The GCE and UCLA/CSU CRMs show a lack of environmental subsidence in the middle troposphere for Subcase C, too. This is related to the underestimate of updraft mass fluxes in these three models (Figure 11). Other consistent features among the models are the lack of environmental subsidence in the lower troposphere and the negative cloud mass flux in the PBL. These features are related to the presence of precipitating downdrafts and the higher cloudbase heights in the CART site than in the tropical oceanic regions (Xu and Randall 2000). A detailed analysis of downdraft characteristics, especially the interaction with the PBL (Krueger et al. 2000), is essential for improving cumulus parameterizations in SCMs/GCMs.

The subcase-mean profiles of updraft and downdraft mass fluxes are shown in Figures 11 and 12, respectively. A striking feature of Figures 11 and 12 is that the intermodel differences are very large, except for the lower troposphere, in spite of the similarity among the profiles. Another significant feature of Figures 11 and 12 is that the two-category ice microphysics (GFDL and EULAG) impacts the diagnosis of updraft and downdraft mass fluxes because these two models produce the lowest values at most heights. Another feature is that 3-D results produce much larger magnitudes of updraft and downdraft mass fluxes in the upper troposphere, which is related to the larger cloud occurrence and

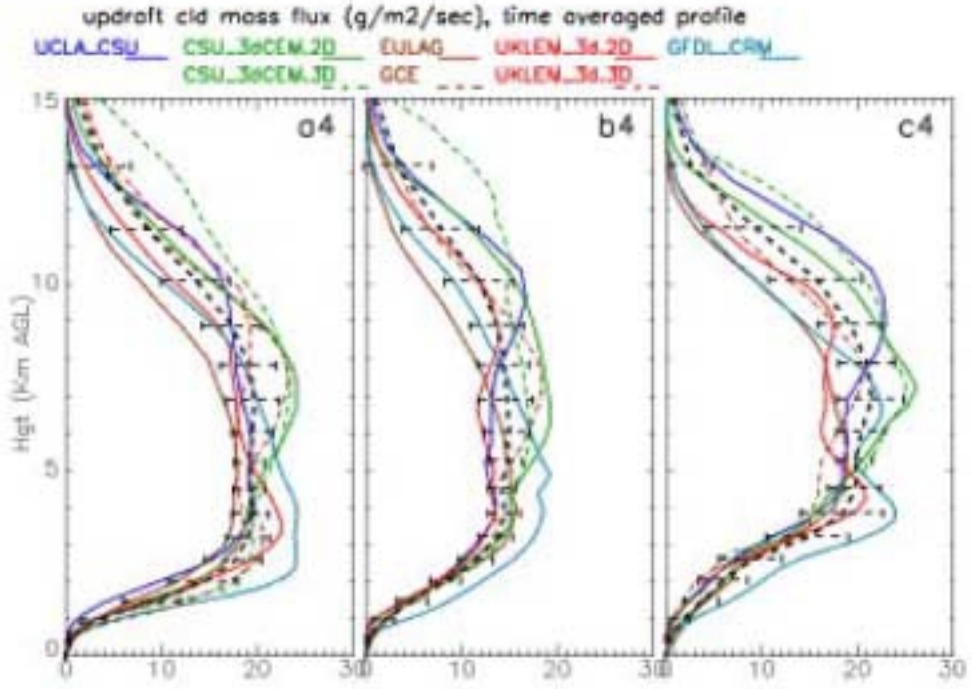

Figure 11. Subcase mean profiles of updraft mass fluxes for Subcases A, B, and C. Mean and standard deviation of all profiles are also shown.

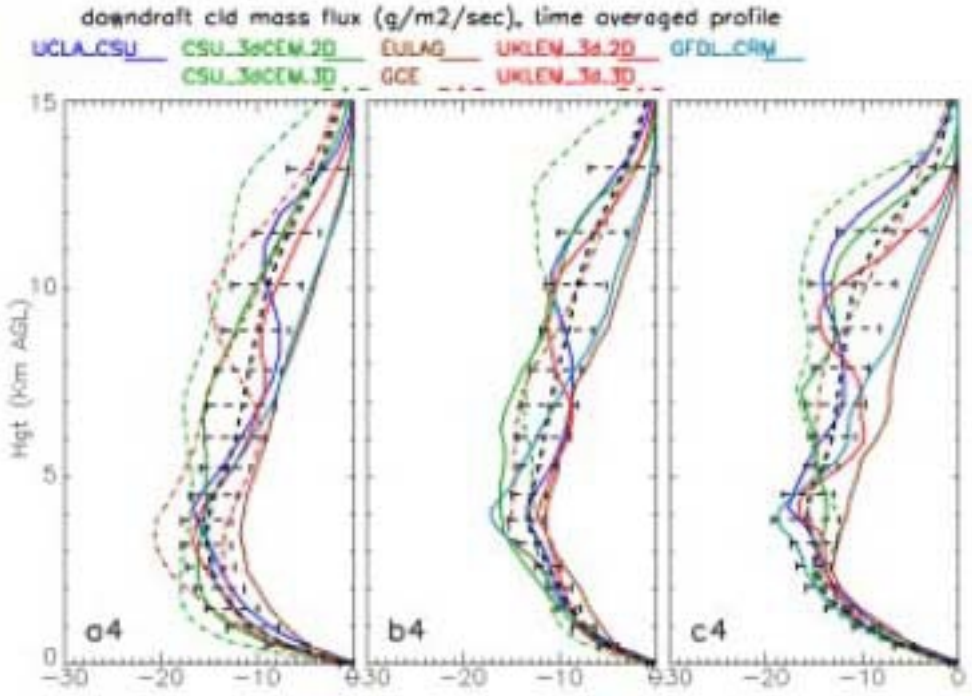

Figure 12. Subcase mean profiles of downdraft mass fluxes for Subcases A, B, and C. Mean and standard deviation of all profiles are also shown.

hydrometeoro fractions shown in Figures 8 and 9. The contributions from gravity-wave reflections are suspected because the magnitudes of both updraft and downdraft mass fluxes are larger. A detailed analysis with trajectory method is needed to narrow down the possible causes for the 2-D and 3-D differences. Another surprising result is the comparable magnitudes in the updraft and downdraft mass fluxes at most heights, which make the net cloud mass flux very small (Figure 10). This feature cannot appear in the simulations of tropical convection (e.g., Xu and Randall 2000).

Discussion

The agreement between simulation and observation is rather remarkable. Some noticeable disagreements are, however, present among the CRMs. For example, the initial convective precipitation events in the CRM simulations of all subcases tend to be delayed relative to observations (Figure 2). Probable causes for this are (1) the lack of initial mesoscale circulations due to initialization from horizontally homogeneous soundings, (2) initial uniform surface fluxes, (3) the lack of spatially non-uniform large-scale advective tendencies, and (4) possible significant errors in the forcing data at times, including the surface turbulent fluxes.

To further understand the differences between simulations and observations and the inter-model differences, further analyses of observations, for example, based upon mesonet measurements, gridded satellite and radar precipitation data, improvements on the variational analysis of the forcing data, e.g., the horizontal moisture advection, and model sensitivity studies will be helpful to reduce the extent of disagreements between models and observations. In addition, some differences between 2-D and 3-D results also need to be further analyzed because 2-D results will be extensively used for improving the representations of cloud processes in SCMs/GCMs.

Summary and Conclusions

In summary, this intercomparison study shows:

- CRMs can reasonably simulate midlatitude continental summer convection observed at the ARM CART site in terms of timing, intensity, temperature and specific humidity evolution.
- The performance of CRMs for simulating midlatitude continental summer convection is comparable to that of tropical oceanic convection, especially the temperature and specific humidity departures from the observations.
- Delayed occurrences of initial precipitation events are a common feature for all three subcases among the CRMs.
- The observed cloud properties are very useful to identify model differences/deficiencies, as well as the differences between 2-D and 3-D results.
- The 2-D results are very close those produced by the 3-D version of the same models; some differences between 2-D and 3-D simulations need to be further examined.

- Cloud mass fluxes produced by all CRMs are rather similar so that they can be used to evaluate SCM/GCM representations of cloud processes.

- The comparable magnitudes in the updraft and downdraft mass fluxes has not been identified with simulations of tropical deep convection.

References

Cahalan, R. F., D. Silberstein, and J. B. Snider, 1995: A validation of a satellite cloud retrieval during ASTEX. *J. Atmos. Sc*i., **52**, 3002-3012.

Cederwall, R. T., and coauthors, 2000: The ARM-GCSS SCM and CRM intercomparison: preliminary SCM results. This proceedings.

Ghan, S. J., and coauthors, 2000: An intercomparison of single column model simulations of summertime midlatitude continental convection. *J. Geophys. Re*s., **105**, 2091-2124.

Grabowski, W. W., X. Wu, M. W. Moncrieff, and W. D. Hall, 1998: Modeling of cloud systems during Phase III of GATE. Part II: Effects of resolution and the third spatial dimension. *J. Atmos. Sc*i., **55**, 3264-3282.

Harshvardhan, B. A. Wielicki, and K. M. Ginger, 1994: The interpretation of remotely sensed cloud properties from a model parameterization perspective. *J. Climat*e, **7**, 1987-1998.

Krueger, S. K., and S. M. Lazarus, 1998: Intercomparison of multi-day simulations of convection during TOGA COARE with several cloud-resolving and single-column models. In *Proceedings of the Eighth Atmospheric Radiation Measurement (ARM) Science Team Meeting*, DOE/ER-0738, pp. 391-397. U.S. Department of Energy, Washington, D.C. Available URL: http://www.arm.gov/docs/documents/technical/conf_9803/krueger(2)-98.pdf

Krueger, S. K., S. M. Lazarus, Y. Luo, and K.-M. Xu, 2000: Interactions of cumulus convection and the boundary layer over the Southern Great Plains. This proceedings.

Liljegren, J. C., 1994: Two-channel microwave radiometer for observations of total column precipitable water vapor and cloud liquid water path. In *Proceedings of the Fifth Symposium on Global Change,* January 23-28, 1994, Nashville, Tennessee, Amer. Meteor. Soc., Boston, Massachusetts, 266-269.

Mace, G. G., E. E. Clothiaux, and T. P. Ackerman, 2000: The composite characteristics of cirrus clouds; bulk properties revealed by one year of continuous cloud radar data. *J. Climat*e (revised July 2000).

Minnis, P., W. L. Smith, Jr., D. P. Garber, J. K. Ayers, and D. R. Doelling, 1995: Cloud properties derived from GOES-7 for Spring 1994 ARM Intensive Observing Period using Version 1.0.0 of ARM satellite data analysis program. *NASA Reference Publication 136*6, NASA Langley Research Center, Hampton, Virginia.

Moran, K. P., B. E. Martner, D. C. Welsh, D. A. Merritt, M. J. Post, and T. Uttal, 1997: ARM's cloud-profiling radar. *28th Conf. on Radar Meteorology*, Austin, Texas, *Amer. Meteor. Soc*.

Petch, J. C., and J. Dudhia, 1998: The importance of the horizontal advection of hydrometeors in a single-column model. *J. Climate*, **11**, 2437-2452.

Redelsperger, J.-L., and coauthors, 2000: A GCSS model intercomparison for a tropical squall line observed during TOGA-COARE. Part I: CRM results. *Quart. J. Roy. Met. Soc*, **115**, 222-2121.

Tompkins, A. M., 2000: The impact of dimensionality on long-term cloud-resolving model simulations. *Mon. Wea. Rev*., **128**, 1521-1535.

Xu, K.-M., and D. A. Randall, 2000: Explicit simulation of midlatitude cumulus ensembles: Comparison with ARM data. *J. Atmos. Sci.,* **57**, 2839-2858.

Zhang, M.-H., and J. L. Lin, 1997: Constrained variational analysis of sounding data based on column-integrated budgets of mass, heat, moisture, and momentum: Approach and application to ARM measurements. *J. Atmos. Sci*., **54**, 1503-1524.